Old and blue white-dwarf stars as a detectable source of microlensing events

Brad M. S. Hansen

Canadian Institute for Theoretical Astrophysics, University of Toronto, Toronto, Ontario M5S 3H8, Canada

The analysis[1] of gravitational microlensing events of stars[2,3] in the Large Magellanic Cloud places the masses of the lensing objects in the range 0.3–0.8 solar masses, suggesting that they might be old white-dwarf stars. Such objects represent the last stage of stellar evolution: they are the cooling cores of stars that have lost their atmospheres after nuclear fusion has ceased in their centres. If white dwarfs exist in abundance in the halo of our Galaxy, this would have profound implications for our understanding of the early generations of stars in the Universe[4–6]. Previous attempts to constrain theoretically[6–8] the contribution of white dwarfs to microlensing indicate that they can account for only a small fraction of the events. But these estimates relied on models of white-dwarf cooling that are inadequate for describing the properties of the oldest such objects. Here I present cooling models appropriate for very old white dwarfs. I find, using these models, that the widely held notion that old white dwarfs are red applies only to those with a helium atmosphere; old white dwarfs with hydrogen atmospheres, which could be a considerable fraction of the total population, will appear rather blue, with colours similar to those of the faint blue sources in the Hubble Deep Field. Observational searches for the population of microlensing objects should therefore look for faint blue objects, rather than faint red ones.

The issue of the observability of old white dwarfs is inextricably linked to the age of the object, because white dwarfs fade with time. The primary uncertainty in the calculation of accurate cooling models is the description of energy transport in the stellar atmosphere, which affects both the cooling rate[9] and observational appearance[10]. Old white dwarfs have luminosities L such that $\log(L/L_\odot) < -4$ and effective temperatures $T_{\rm eff} < 6{,}000$ K (here $L_\odot$ is the solar luminosity). The atmospheric constituents at these temperatures are neutral, so that the primary opacity sources are the collisionally induced absorption of molecular hydrogen (for hydrogen atmospheres) or Rayleigh scattering (for helium atmospheres). The molecular opacities are strongly wavelength-dependent and require a detailed radiative transfer calculation. The calculation of such atmosphere models[10] has led to advances in the study of the basic physical parameters of old white dwarfs[11]. However, previous cooling models have used outer boundary conditions calculated using simplified atmosphere calculations, so that the self-consistent determination of cooling ages from atmospheric models was not possible for the oldest white dwarfs. The cooling models described here aim to rectify that uncertainty.

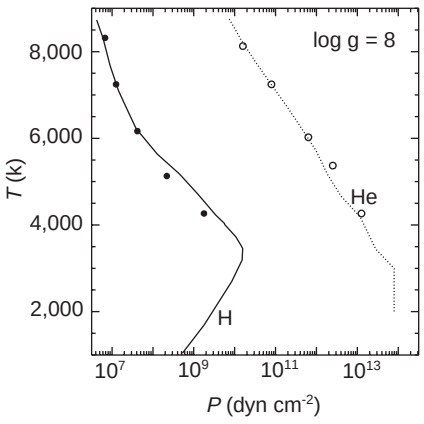

Figure 1 Location of the photosphere in white dwarfs. The solid and dotted lines indicate the evolution of the photospheres for hydrogen and helium atmospheres respectively. The solid and open circles are the same quantities from the work of Bergeron *et al.*[10].

My calculations use a white-dwarf cooling model originally developed for the study of the companions to millisecond pulsars[12]. To this I have added a detailed atmospheric model using the Feautrier and Avrett-Krook methods[13] to solve the radiative transfer at the surface. The atmospheric model provides an outer boundary condition (taken to be the photosphere) for the interior model which describes the cooling of the white dwarf. The position of the photosphere for helium and hydrogen atmospheres differs dramatically, because neutral helium does not form molecules so that the opacity κ is much lower and hence the density at the photosphere $\rho \propto 1/\kappa T_{\rm eff}$ is much larger. Figure 1 shows the location of the photosphere for hydrogen and helium atmospheres, respectively. In both cases, the photospheric density increases as the star cools and $T_{\rm eff}$ drops. This trend ends when both atmospheres reach $T_{\rm eff} \approx 3{,}000$ K, but for different reasons. For helium atmospheres, pressure ionization of helium increases the opacity dramatically, halting the inward motion of the photosphere. For hydrogen atmospheres, the molecular hydrogen opacity is stronger at long wavelengths $\lambda > 1\ \mu$m, so that the opacity increases when the peak of the black-body $\lambda_{\rm ob} \approx 1.7\ \mu{\rm m}/(T_{\rm eff}/3{,}000\ {\rm K})$ moves into that range, and hence the photospheric density moves outwards again. The molecular opacity is strongly wavelength-dependent, so that the observational appearance of these old stars deviates significantly from a black-body spectrum, in a similar fashion to that seen in brown-dwarf atmospheres[14].

Figure 2 shows the comparison of the cooling results with the best models in the literature[15,16]. The agreement with the hydrogen-atmosphere models is excellent until the models reach $T_{\rm eff} \approx 6{,}000$ K, at which point my improved treatment of the

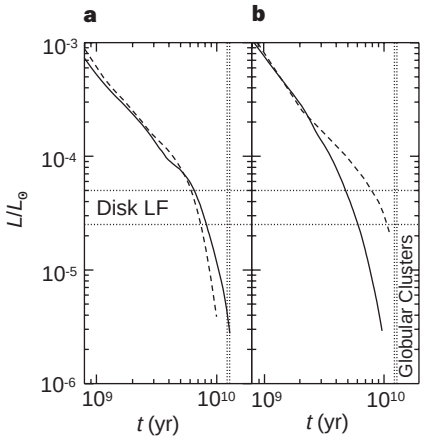

Figure 2 Calculated cooling curves. **a**, Comparison of this work (solid line) with the models of Wood[15] (dashed line). The model is for a $0.6M_\odot$ white dwarf with an oxygen core, and a hydrogen mass fraction of 10^{-4}. The improved boundary condition leads to a slight flattening of the cooling curve at $\log L/L_\odot \approx -4$ and longer cooling times thereafter. **b**, Comparison of this work (solid line) with the model of Salaris *et al.*[16] (dashed line). The model is for a $0.6M_\odot$ carbon/oxygen model with a helium mass fraction of $10^{-3.25}$. The much longer cooling of the Salaris model is because of the outdated atmospheric model used in that work. In both panels, the horizontal dotted lines enclose the location of the turnover in the disk white-dwarf luminosity function (LF). The vertical dotted lines indicate the mean age of the globular clusters[27], indicating the expected age of any halo white-dwarf population. The large variations in the different models at these ages indicate how important are accurate atmosphere models.

atmospheric physics results in slower cooling. The difference in the helium models is more dramatic, with the new models cooling rather more rapidly. This is a result of the extremely low opacity of neutral helium. Application of the new models to the white-dwarf luminosity function shows that previous age estimates for Galactic disk hydrogen dwarfs were reasonably accurate, although disk helium dwarf ages were somewhat overestimated. However, for white dwarfs residing in the Galactic halo or in globular clusters, the differences are very important. In particular, previous efforts to place constraints on white-dwarf dark matter[6–8] have been unduly pessimistic because they use inappropriate white-dwarf models.

The observational constraints on local white-dwarf dark matter centre on two sources, the luminosity function determined from proper motions[17] and searches for point sources in the Hubble Deep Field[18–20]. Unfortunately, the proper-motion sample suffers from poorly constrained incompleteness at the fainter magnitudes (the luminosity function declines much more rapidly than the luminosity function based on white dwarfs in binaries[21]). Thus, inferring how many objects could have been seen at fainter magnitudes may lead to erroneous results. More robust estimates must rely on the Hubble Deep Field (HDF) alone. Figure 3 shows the point sources detected in the HDF by various workers, along with cooling tracks for both hydrogen and helium atmospheres. The first result that one can glean from this is that the HDF places no limits on helium-atmosphere dwarfs, because the rapid cooling means that they become unobservable within 6 Gyr, which is approximately half their expected age. The second and most interesting result is that the hydrogen-atmosphere dwarfs are potentially observable and would lie in the region of the faint blue objects that were indeed detected. This is contrary to the conventional wisdom which states that white dwarfs should become redder with age because that is the trend shown by a black body (and indeed that is what happens to the helium dwarfs). The deviation towards the blue shown by the hydrogen-atmosphere dwarfs is again a consequence of the strong molecular hydrogen opacity which also causes the photosphere to move to lower densities in Fig. 1. The strong opacity at longer wavelengths (red) forces the stellar flux to emerge at shorter wavelengths (blue) where the opacity is smaller. Thus, hydrogen atmosphere white dwarfs may have already been detected in the halo.

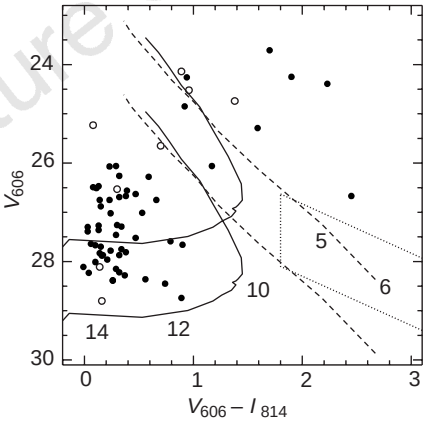

Figure 3 Stellar objects in the Hubble Deep Field. The filled circles are the unresolved objects detected by Elson *et al.*[19]; the open circles are the point sources from Mendez *et al.*[20]. Although Flynn *et al.*[18] did not publish a table of detections, the dotted line encloses their 'halo region', which they used to constrain the halo white-dwarf population. The dashed lines show the cooling behaviour of a helium atmosphere white dwarf at a distance of 1 kpc (upper line) and 2 kpc (lower line). The upper curve is labelled with ages in Gyr at appropriate points. The solid lines represent the corresponding evolution of a hydrogen-atmosphere dwarf at 1 and 2 kpc. The dwarf ages are shown on the lower curve in this case. The bandpasses are the Hubble Telescope bandpasses from Holtzman *et al.*[28]. The blueward shift for ages 10–12 Gyr is due to the presence of molecular hydrogen in the atmosphere.

To connect quantitatively these findings to the observational searches, one also requires a model for the relative populations of hydrogen- and helium-atmosphere white dwarfs. Recent advances in asteroseismological investigations of white dwarfs[22] have confirmed that many hydrogen-atmosphere white dwarfs have hydrogen surface layers of mass $\sim 10^{-4}\,M_{\odot}$ (here $M_{\odot}$ is the solar mass). This suggests that such stars will survive as hydrogen-atmosphere dwarfs despite the mixing effects of surface convection zones. Although these estimates are for disk white dwarfs, the mechanisms for removing hydrogen from the surface of a white dwarf[9,23,24] should become less efficient in stars with lower metallicity, such as those in the halo and in globular clusters. The relative proportion of hydrogen atmospheres amongst the cool white dwarfs in the disk appears to be >50%, so I will adopt this as a conservative estimate. In the future, the effect of advanced age and lower progenitor metallicity could be empirically tested by examining the faint white dwarfs in globular clusters[25].

How many white dwarfs would one expect to see in the Hubble Deep Field? The HDF probes great distances, but only over a very small portion of sky, so that the total Galactic volume sampled is quite small. Given a limiting V-band magnitude $m_V \approx 28$ and an absolute magnitude for old white dwarfs $M_V \approx 17$, the corresponding volume probed is only:

$$V_{\mathrm{HDF}} \approx (5.4\,\mathrm{pc})^3 10^{0.6((m_V - 28) - (M_V - 17))}$$

Thus, even if the white dwarfs constitute the entire local dark matter ($\sim 0.01\,M_{\odot}\,\mathrm{pc}^{-3}$; ref. 26), their space density is only $\sim 0.02\,\mathrm{pc}^{-3}$ and hence we expect to find only three, even if all the white dwarfs have hydrogen atmospheres and are 12 Gyr old (an age appropriate for globular cluster and halo stars). Our most realistic estimate invokes only 50% of the total number in hydrogen-atmosphere white dwarfs and requires that only 50% of the dark matter is in the form of white dwarfs[1]. In this case, the volume probed by the HDF is too small to reliably detect even one object. Nevertheless, as one can see in Fig. 3, several point sources have been detected in the HDF. Given the relative profusion of these objects, most must have another origin, such as extragalactic star-forming regions[19].

These results have two implications for the search for dark matter. The first is that deep surveys for very red objects are unlikely to be successful in the near future because the red population (helium-atmosphere dwarfs) will be very faint. However, searches for faint blue objects could be much more successful. The second implication is that the hydrogen-atmosphere dwarfs are observable, but that the HDF results suggest that there are other unresolved populations of objects with similar colours and magnitudes. Thus determinations of proper motions will be essential, to distinguish Galactic from extragalactic objects. □

Received 30 March; accepted 8 June 1998.

1. Alcock, C. *et al.* The MACHO project Large Magellanic Cloud microlensing results from the first two years and the nature of the Galactic dark halo. *Astrophys. J.* **486,** 697–726 (1997).
2. Alcock, C. *et al.* Possible gravitational microlensing of a star in the Large Magellanic Cloud. *Nature* **365,** 621–623 (1993).
3. Aubourg, E. *et al.* Evidence for gravitational microlensing by dark objects in the galactic halo. *Nature* **365,** 623–625 (1993).
4. Larson, R. B. Dark matter—dead stars? *Comments Astrophys.* **11,** 273–282 (1987).
5. Charlot, S. & Silk, J. Signatures of white dwarf galaxy halos. *Astrophys. J.* **445,** 124–132 (1995).
6. Adams, F. & Laughlin, G. Implications of white dwarf galactic halos. *Astrophys. J.* **468,** 586–597 (1996).
7. Chabrier, G., Segretain, L. & Mera, D. Contribution of brown dwarfs and white dwarfs to recent microlensing observations and the halo mass budget. *Astrophys. J.* **468,** L21–L24 (1996).
8. Graff, D. S., Laughlin, G. & Freese, K. MACHOs, white dwarfs and the age of the universe. *Astrophys. J.* **499,** 7–19 (1998).
9. D'Antona, F. & Mazzitelli, I. Cooling of white dwarfs. *Annu. Rev. Astron. Astrophys.* **28,** 139–181 (1990).
10. Bergeron, P., Saumon, D. & Wesemael, F. New model atmospheres for very cool white dwarfs with mixed H/He and pure He compositions. *Astrophys. J.* **443,** 764–779 (1995).
11. Bergeron, P., Ruiz, M. T. & Leggett, S. K. The chemical evolution of cool white dwarfs and the age of the local galactic disk. *Astrophys. J. Suppl.* **108,** 339–387 (1997).
12. Hansen, B. M. S. & Phinney, E. S. Stellar forensics I: cooling curves. *Mon. Not. R. Astron. Soc.* **294,** 557–568 (1998).

13. Mihalas, D. *Stellar Atmospheres* (Freeman, San Francisco, 1970).
14. Saumon, D., Bergeron, P., Lunine, J. I., Hubbard, W. B. & Burrows, A. Cool zero-metallicity stellar atmospheres. *Astrophys. J.* **424,** 333–344 (1994).
15. Wood, M. A. in *White Dwarfs* (eds Koester, D. & Werner, K.) 41 (Springer, Heidelberg, 1995).
16. Salaris, M. *et al.* The cooling of CO white dwarfs: influence of the internal chemical distribution. *Astrophys. J.* **486,** 413–419 (1997).
17. Liebert, J., Dahn, C. D. & Monet, D. G. The luminosity function of white dwarfs. *Astrophys. J.* **332,** 891–909 (1988).
18. Flynn, C., Gould, A. & Bahcall, J. N. Hubble Deep Field constraint on baryonic dark matter. *Astrophys. J.* **466,** L55–L58 (1996).
19. Elson, R. A. W., Santiago, B. X. & Gilmore, G. F. Halo stars, starbursts, and distant globular clusters: A survey of unresolved objects in the Hubble Deep Field. *New Astron.* **1,** 1–16 (1996).
20. Mendez, R. A., Minniti, D., de Marchi, G., Baker, A. & Couch, W. J. Starcounts in the Hubble Deep Field: constraining galactic structure models. *Mon. Not. R. Astron. Soc.* **283,** 666–672 (1996).
21. Oswalt, T. D., Smith, J. A., Wood, M. A. & Hintzen, P. A lower limit of 9.5 Gyr on the age of the galactic disk from the oldest white dwarf stars. *Nature* **382,** 692–694 (1996).
22. Clemens, J. C. The pulsation properties of the DA white dwarf variables. *Baltic Astron.* **2,** 407–434 (1993).
23. Iben, I. A. & MacDonald, J. The effects of diffusion due to gravity and due to composition gradients on the rate of hydrogen burning in a cooling degenerate dwarf. I. The case of a thick helium buffer layer. *Astrophys. J.* **296,** 540–553 (1985).
24. Paczynski, B. Evolution of single stars. VI. Model nuclei of planetary nebulae. *Acta Astron.* **21,** 417–435 (1971).
25. Richer, H. B. *et al.* White dwarfs in globular clusters: Hubble Space Telescope observations of M4. *Astrophys. J.* **484,** 741–760 (1997).
26. Bahcall, J. N., Schmidt, M. & Soneira, R. M. The galactic spheroid. *Astrophys. J.* **265,** 730–747 (1983).
27. Chaboyer, B., DeMarque, P., Kernan, P. J. & Krauss, L. M. The age of globular clusters in the light of Hipparcos: resolving the age problem? *Astrophys. J.* **494,** 96–110 (1998).
28. Holtzman, J. A. *et al.* The photometric performance & calibration of WFPC2. *Publ. Astron. Soc. Pacif.* **107,** 1065–1093 (1995).

Acknowledgements. I thank the Aspen Center for Physics for hospitality, and M. Wood, G. Chabrier, E. Garcia-Berro and M. Hernanz for comments.

Correspondence and requests for materials should be addressed to the author (e-mail: hansen@cita.utoronto.ca).

A symmetrically pulsed jet of gas from an invisible protostar in Orion

Hans Zinnecker*, Mark J. McCaughrean* & John T. Rayner†

* *Astrophysikalisches Institut Potsdam, An der Sternwarte 16, 14482 Potsdam, Germany*
† *Institute for Astronomy, University of Hawaii, 2680 Woodlawn Drive, Honolulu, Hawaii 96882, USA*

Young stars are thought to accumulate most of their mass through an accretion disk, which channels the gas and dust of a collapsing cloud onto the central protostellar object[1]. The rotational and magnetic forces in the star–disk system often produce high-velocity jets of outflowing gas[2–6]. These jets can in principle be used to study the accretion and ejection history of the system, which is hidden from direct view by the dust and dense gas of the parent cloud. But the structures of these jets are often too complex to determine which features arise at the source and which are the result of subsequent interactions with the surrounding gas. Here we present infrared observations of a very young jet driven by an invisible protostar in the vicinity of the Horsehead nebula in Orion. These observations reveal a sequence of geyser-like eruptions occurring at quasi-regular intervals and with near-perfect mirror symmetry either side of the source. This symmetry is strong evidence that such features must be associated with the formation of the jet, probably related to recurrent or even chaotic instabilities in the accretion disk.

The infrared and millimetre continuum source IRAS05413–0104 is a cold (~30 K), low-luminosity (~15 times the solar luminosity) young protostar[7–9]. The molecular cloud core in which it is embedded has a typical gas density of $\sim 10^4\,cm^{-3}$, but the exceptionally low turbulent velocity dispersion[10] and presence of strong water maser emission[7,11] at 1.3 cm wavelength single it out as unusual compared to others in Orion[7,8,10].

Initial near-infrared observations of the core, using an infrared camera with a small field of view, showed a pair of bright sources interpreted as a young binary stellar system[12]. However, subsequent observations showed them to be the innermost of a linear chain of knots at the base of a large jet of shocked molecular hydrogen (H_2) gas. Figure 1 shows the jet, now named HH212—for Herbig–Haro object 212 (ref. 13)—in the rotational–vibrational $v = 1$–0 S(1) emission line of H_2 at a wavelength of 2.122 μm. Strong H_2 emission is often seen from young jets[14], although it does not delineate the bulk jet fluid, but rather shows radiative cooling from shocks where the fluid interacts with itself or with the ambient molecular cloud. Fortunately, many bright H_2 lines are found at near-infrared wavelengths where the extinction is relatively low, thus allowing us to study young jets still embedded in their dusty natal material. Spectroscopy (Fig. 2) demonstrates that the 1.62–2.42 μm emission from HH212 is almost exclusively in lines of shocked H_2 at an excitation temperature of ~2,400 K, with just the tips of the brightest knots also exhibiting higher excitation [Fe II] emission at 1.644 μm. No evidence is seen for the Brγ line of ionized hydrogen at 2.166 μm, although for a typical ionized jet, the estimated Brγ surface brightness would be factors of ~10–100 below the current detection limit. Thus, nothing definitive can be said about the ionization fraction in HH212 based on the present data, although because it is one of the few jet sources not showing 3.6 cm radio continuum emission from ionized gas[15], the jet fluid may be predominantly molecular.

High-resolution spectroscopy of the two centre knots (Fig. 2) shows only a small velocity shift of $\sim 9\,km\,s^{-1}$ between them, implying that the flow lies within ~1° of the plane of the sky, assuming a velocity of $200\,km\,s^{-1}$ typical for young stellar jets[16,17]. Thus any circumstellar disk around the central source must be seen nearly edge-on. Such a geometry, combined with the extended dense envelope normally associated with a protostar, explains the invisibility of the central source at these short wavelengths. The disk and envelope—as well as outflowing CO and SiO molecules in the jet—are seen directly in millimetre interferometry observations (K. B. Marvel, M.J.McC and A. I. Sargent, manuscript in preparation), while at near-infrared continuum wavelengths, two faint broad parabolic nebulae appear to delineate the concave surfaces of the disk/envelope illuminated by light reflected from the central source, as in the HH30 disk/jet system[18].

HH212 covers a total length of ~240 arcsec, or ~0.5 pc (~10^5 AU) at the 400-pc distance to the parent molecular cloud, and shows a remarkable bipolar symmetry centred on the driving source (Fig. 1b). A series of knots is seen near the source, mostly in pairs positioned at equal distances on the two sides (NK1–7 and SK1–7). These inner knots are all resolved, with intrinsic diameters of ~250–500 AU; they are wider transverse to the jet axis than parallel to it and convex in the direction of the outflow, and thus are probably small bow shocks in the flow. Further out, where the jet appears to leave the confines of the gas core[10], the first of the chief bow shocks are seen; these are symmetric even to the extent that both are split into two components (NB1/2 and SB1/2). Beyond these, a pair of large, fully developed bow shocks is seen (NB3 and SB3), until finally the gross symmetry is broken by another large bow on the south side (SB4) which has no northern counterpart (as searched for in wider-field images than shown here). The pairs of features are generally equidistant from the centre to within 5–15%, with two distinct scale lengths involved (Table 1): the spacing of the brighter inner knots is ~2,000 AU, whereas the larger bow shock systems are at ~16,000–18,000 AU intervals. Again assuming a constant jet outflow velocity of $200\,km\,s^{-1}$, these distances correspond to timescales of ~50 and 500 years, respectively.

HH212 is by far the most symmetric jet found to date, compared to systems such as the rather complex HH47[19], or even the more regular HH111, where some symmetry is seen[20,21]. In HH212, even the deviations from perfectly regular spacing are also symmetric about the centre. If symmetry is an inherent part of the jet-